Measurements of Turbulence at Two Tidal Energy Sites in Puget Sound, WA

Jim Thomson, Brian Polagye, Vibhav Durgesh, and Marshall C. Richmond

***Abstract*—Field measurements of turbulence are presented from two sites in Puget Sound, WA, that are proposed for electrical power generation using tidal current turbines. Time series data from multiple acoustic Doppler instruments are analyzed to obtain statistical measures of fluctuations in both the magnitude and direction of the tidal currents. The resulting turbulence intensities (i.e., the turbulent velocity fluctuations normalized by the deterministic tidal currents) are typically 10% at the hub heights (i.e., the relevant depth) of the proposed turbines. Length and time scales of the turbulence are also analyzed. Large-scale, anisotropic eddies dominate the turbulent kinetic energy (TKE) spectra, which may be the result of proximity to headlands at each site. At small scales, an isotropic turbulent cascade is observed and used to estimate the dissipation rate of TKE, which is shown to balance with shear production. Data quality and sampling parameters are discussed, with an emphasis on the removal of Doppler noise from turbulence statistics. The results are relevant to estimating the performance and fatigue of tidal turbines.**

***Index Terms*—Acoustic Doppler current profiler (ADCP), acoustic Doppler velocimeter (ADV), marine and hydrokinetic energy, tidal energy, tidal power, turbulence, turbulence intensity.**

I. Introduction

THE successful development of turbines to generate electricity from tidal currents requires detailed knowledge of the inflow conditions. Computational or laboratory models are able to simulate the basic flows, however it is not possible, at present, to directly model the turbulence at all of the relevant scales. Rather, the turbulence must be estimated from field observations of the flow, which are inherently sparse and noisy. This paper presents field observations from two tidal energy sites and then evaluates a set of turbulence metrics. The focus is on ambient turbulence (i.e., natural turbulence before the installation of turbines) and the goal is to provide characteristic design conditions for tidal turbines.

In the analogous case of observations at wind energy sites, the key parameters are the turbulence intensity (ratio of velocity fluctuations to velocity mean) and the turbulence spectra (velocity variance as a function of frequency) measured at turbine hub height (i.e., the axis of the turbine). These parameters have been shown to correlate with turbine performance and structural fatigue, with distinct contributions from: naturally occurring turbulence, ambient increases within a wind farm, and the wakes of individual turbines [1]. More detailed analyses of coherent turbulence have also been introduced [2], [3].

Information about turbulence is essential to optimizing the design of wind or water turbines. Performance and design codes require information about the 3-D structure of turbulence. For example, the FAST code developed by the National Renewable Energy Laboratory (Washington, DC), is an unsteady aerostructural code forced by the TurbSim model, which is a turbulent (coherent and incoherent) simulator initialized with field measurements. These, and other, design codes have helped the wind industry reach its present state of maturity and reliability. Leveraging this experience would benefit tidal energy development, but a critical gap in developing comparable design codes for tidal turbines is a lack of information about ambient turbulence.

There have been few observations of naturally occurring tidal turbulence and no observations of turbulence within a turbine farm (all but one of the installations worldwide have been single device demonstrations). Of the previous tidal studies, most have focused on the hydrodynamics of the turbulent kinetic energy (TKE) budget, rather than the inflow conditions for turbines. Beginning with an early observational study to confirm the theoretical turbulent energy cascade at small scales [4], several studies have evaluated the key dynamics quantities of turbulent shear production, dissipation rate, and transport [5]–[10]. A key aspect of these studies has been error correction from acoustic Doppler measurements of velocity. Recent work has also addressed the utility (and limitations) of similarity theory in TKE spectra in tidal channels [11].

Recently, studies of more direct relevance to tidal turbines have been published. Observations from the European Marine Energy Centre (United Kingdom) have been used to evaluate Reynolds stresses, TKE density, the rates of TKE production and dissipation, and the local eddy viscosity [12]. Previous observations from a tidal energy site in Puget Sound, WA, have been used to assess turbulence intensity and demonstrate the importance of accounting for instrument error (i.e., "noise") from acoustic Doppler measurements [13]. Here, we extend those techniques to a new, more extensive, data set, including a second site, and examine the time and length scales of the naturally occurring turbulence. The emphasis is on providing the best statistical description of the natural inflow conditions for tidal turbines and the results are restricted to turbine hub heights for consistency with wind energy literature [1]. Evaluation of the TKE budget is included, however it is largely to evaluate data

Manuscript received August 26, 2011; revised December 20, 2011; accepted March 14, 2012. Date of publication May 15, 2012; date of current version July 10, 2012. This work was supported by the U.S. Department of Energy, Office of Energy Efficiency and Renewable Energy—Wind and Water Power Program.

Associate Editor: H. Maeda.

J. Thomson and B. Polagye are with the Northwest National Marine Renewable Energy Center, University of Washington, Seattle, WA 98195-2600 USA (e-mail: jthomson@apl.washington.edu).

V. Durgesh and M. C. Richmond are with the Hydrology Group, Pacific Northwest National Laboratory, Richland, WA 99352 USA.

Digital Object Identifier 10.1109/JOE.2012.2191656

quality and noise corrections, rather than investigate the hydrodynamics. Predictions of actual electricity production and description of the overall site characteristics are given in [14] and [15]. These turbulence measurements represent an important step in the development of robust design tools that will improve the survivability, reliability, and performance of tidal turbines.

A. Decomposition of Velocity Components

We present field observations of tidal currents from two sites and decompose the observed horizontal currents into

$$\mathbf{u}(z) = \bar{\mathbf{u}} + \tilde{u} + u'. \tag{1}$$

The velocity vector $\mathbf{u}$ is defined from components $u\hat{i} + v\hat{j}$, which are along and across the principal axis of the tidal flow, respectively, and vary with distance above the seabed z. The field observations are fixed in space, and thus variations in $[x, y]$ are neglected. (For a description of spatial variations at tidal power sites, see [16].)

Here, $\bar{\mathbf{u}}$ is the background (deterministic) tidal flow that can be modeled using harmonic constituents [17], but may also contain local aharmonic currents [18], [14]. This background flow is nearly constant on short time scales (i.e., minutes). The $\tilde{\mathbf{u}}$ velocities are flows resulting from external forcing, such as wind- and density-driven (estuarine) flows [19], or surface-wave orbital velocities, which decay beneath the surface as $\cosh(kz)/\cosh(kh)$, where the wave number k is from linear theory, z is the distance above the seabed, and h is the total water depth [20]. Finally, the $\mathbf{u}'$ are turbulent velocity fluctuations, which span length and time scales from large eddies to small isotropic turbulence [21], [22]. The statistical treatment of these fluctuations is the focus of this paper.[1]

In addition to fluctuations of velocity magnitude $u' = |\mathbf{u}'|$, we examine fluctuations of direction θ' from the principal axis of the tidal flow. Directional fluctuations may be important for the yaw control of a turbine, or off-axis power projections in the case of a fixed-yaw turbine. Analyses include the relative intensity of these fluctuations, the frequency spectra and length scales of these fluctuations, and the dynamic balance of turbulence production dissipation. The focus is on the horizontal component of the currents, as those are most relevant to tidal turbines, and, as shown in the analysis (Section III-D), the horizontal currents contain the majority of the TKE, compared with the vertical currents.

II. Data Collection

A. Instruments and Sampling Considerations

The tidal currents are measured using acoustic Doppler instruments, which estimate the flow speed by evaluating the Doppler shift of acoustic pulses along different axes. Acoustic Doppler velocimeters (ADVs) sample a small volume [O(1 cm) diameter] using three (or sometimes four) convergent acoustic beams to infer three components of velocity at a point. Acoustic Doppler current profilers (ADCPs) sample larger volumes [O(1 m) diameter] over a set of range bins using three (or sometimes four) divergent acoustic beams to infer three components of velocity at multiple points along a profile.[2] Both instruments have intrinsic standard errors n, which result from estimating the Doppler shift of finite-length acoustic pulses and are termed "Doppler noise" [23]. The Doppler noise is typically much larger for ADCPs than for ADVs, and often many measurements, or "pings," of ADCP data are averaged to reduce the standard error. However, for turbulence calculations, averaging obscures the velocity variance. Instead, the raw pings must be retained, and Doppler noise must be removed from the velocity variance statistically [5], [6], [9], [24], [13]. For measurements of tidal energy sites, bottom-mounted ADCP deployments are far more practical than hub-height ADV measurements. The practicality is at the expense of increased Doppler noise n and larger sampling volumes. The measurements herein compare a collocated ADV and ADCP, as well as ADCPs with varied sampling parameters, to quantify the impact of Doppler noise in calculating turbulence statistics.

In choosing sampling parameters for an ADCP, there is a tradeoff between longer pulses (i.e., larger range bins) with lower Doppler noise and shorter pulses (i.e., smaller range bins) with higher Doppler noise. For example, smaller bins will give spuriously larger raw turbulence intensities even in the case of perfect steady flow (with no true turbulent fluctuations). Since the theoretical corrections for Doppler noise are imperfect (see Section III), it is preferable to choose the largest bins tolerable (and thus reduce the amount of noise that must be later removed from the turbulence statistics). One option for choosing a sampling scheme is to require Doppler noise values that are notably smaller than the expected turbulent fluctuations u', based on *a priori* knowledge of the tidal flow $\bar{u}$ and a canonical turbulence intensity $I_u \approx 10\%$ [13]. Another option is to set the bin size to be the minimum resolution required for determining vertical shear of the mean flow $d\bar{u}/dz$.

In addition to a dependence on bin size (via pulse length), the Doppler noise of ADCP measurements depends on sampling rate f_s. The sampling rate determines the number of raw pings N that are averaged per velocity value, and the Doppler noise is reduced by a factor $\sqrt{N}$. Time averaging can be used in postprocessing to reduce Doppler noise, at the expense of temporal resolution. However, temporal resolution is essential to capture the turbulent fluctuations. An appropriate sampling rate f_s can be determined by considering the frequency f at which a horizontal eddy with a length scale similar to the beam spread Δb will appear when advected by the tidal flow $\bar{u}$, according to Talyor's "frozen field" hypothesis

$$f_s = \frac{\bar{u}}{\Delta b}. \tag{2}$$

In practice, f_s should be twice this estimate to avoid aliasing, but may be limited by the instrument. For isotropic turbulence, the vertical bin size Δz could be substituted for the beam spread Δb in (2), and along-beam velocity fluctuations could be analyzed. However, horizontal fluctuations are most relevant to

[1]Note that magnitude fluctuations, as opposed to component fluctuations, are used for consistency with wind energy studies. An important consequence, for interpretation and comparison of results, is that the variance in the magnitude will be less than the sum of variances in the components.

[2]ADCP is a common term from the manufacturer Teleydyne RDI (Poway, CA). The acoustic wave and current meter (AWAC) is similar instrument from Nortek (Oslo, Norway), and the same sampling considerations apply.

TABLE I
SUMMARY OF DEPLOYMENT LOCATIONS, SAMPLING PARAMETERS, AND DOPPLER NOISE

Site	Nodule Point	Nodule Point	Admiralty Head	Admiralty Head
Instrument	Nortek Vector ADV	RDI Workhorse ADCP	Nortek AWAC	Nortek AWAC
Frequency [MHz]	6.0	0.6	1.0	1.0
Lat	N 48 01.924'	N 48 01.924'	N 48 09.141'	N 48 09.088'
Lon	W 122 39.689'	W 122 39.689'	W 122 41.300'	W 122 41.129'
h [m]	22	22	62	56
z [m]	4.7	3.2-20.6	1.1-20.1	1.1-20.1
T [days]	4.3	17	11	32
f_s [Hz]	32	2	1	1
N [pings]	1	1	7	7
Δz [m]	n/a	0.5	0.5	1.0
u_{amb} [m/s]	2.0	2.0	n/a	n/a
n [m/s]	0.02	0.156	0.224	0.112
z_{hub} [m]	4.7	4.7	8.1	8.1
Δb_{hub} [m]	n/a	2.6	6.8	6.8

tidal turbines, and these fluctuations require information from multiple ADCP beams. Thus, the beam spread is the limiting length scale. Either way, the goal is to restrict analysis to length scales (and corresponding frequencies) that are accurately measured by the instrument. The beam spread Δb increases with distance from the instrument, so this requirement will be more restrictive for hub heights farther above the seabed (assuming a bottom-mounted ADCP).

The sampling parameters used in this study are shown in Table I, including the sampling frequency f_s, the number of raw pings averaged N, the bin resolution Δz, and the Doppler ambiguity velocity $u_{\rm amb}$ [23]. Analysis at each site uses a hub height ($z_{\rm hub}$, distance above the seabed) that is specific to the turbine proposed for that site. The corresponding beam spread Δb (horizontal distance) at hub height also is given in Table I. For the first site (Nodule Point), collocated ADV and ADCP measurements provide a direct comparison of observations with different Doppler noise. For the second site (Admiralty Head), sequential AWAC[2] measurements provide an indirect comparison of observations with different Doppler noise by varying the sampling parameters. The Doppler noise values shown in Table I are obtained from the instrument manufacturers' deployment software, and potential biases from these values are discussed in Section III-A.

Since time averaging can be done in postprocessing, the raw ADCP and AWAC data were recorded to maintain maximum flexibility in data analysis. This is in contrast to bin size (i.e., the pulse length), for which the Doppler noise dependence cannot be modified in postprocessing by averaging vertical bins, because the Doppler shift of pulses is computed onboard the instrument. Doppler noise is also a function of acoustic pulse frequency, and higher frequency profilers are preferred, subject to range limitations (see Table I).

B. Sites

Fig. 1 shows the sites, along with the instruments and platforms used. Additional site details are presented in Table I, including the total depth at the site h and the turbine hub height ($z_{\rm hub}$, distance above the seabed) that is specific to the turbine proposed for that site.

Nodule Point, on the eastern side of Marrowstone Island, is the proposed location for a small array of Verdant Power™ turbines as a demonstration project by the U.S. Navy. Velocity profiles were collected from February 10 to February 17, 2011, using an ADCP mounted on a leg of the Tidal Turbulence Tripod (Fig. 1). In addition, high-precision velocity measurements were collected during the spring tide from February 17 to February 21, 2011, using an ADV mounted at the apex of the Tidal Turbulence Tripod, 4.7 m above the seabed. The ADV has a substantially lower Doppler noise n (see Table I) and thus can be used to evaluate noise-corrected estimates from the ADCP. For the purpose of data analysis, a turbine hub height of 4.7 m above the seabed is assumed, which is within 1 m of the proposed hub height (still to be determined by Verdant Power™). The site is 22 m deep and has a maximum hub-height current $\bar{u}(z_{\rm hub}) = 1.8$ m/s.

Admiralty Head, on the western side of Whidbey Island, is the proposed location for two OpenHydro™ turbines as a pilot project by the Snohomish Public Utility District. Velocity profiles were collected in two deployments of an AWAC mounted on a Sea Spider (Fig. 1): from February 10 to February 21, 2011 and from May 9, 2011 to June 8, 2011. The change in sampling parameters from the first to the second deployment (increase in bin size, and thus pulse length) resulted in a lower Doppler noise n (see Table I). The variation in Doppler noise can be used to evaluate the robustness of postprocessing noise correction (assuming similar conditions between the two deployments). For the purpose of data analysis, a turbine hub height of 8.1 m above the seabed is assumed, which is within 1 m of the proposed hub height (still to be determined by OpenHydro™). The site is 56 m deep and has a maximum hub-height tidal current of $\bar{u}(z_{\rm hub}) = 3.2$ m/s.

Both sites are in close proximity to headlands, which can cause flow separation and produce large eddies, depending on

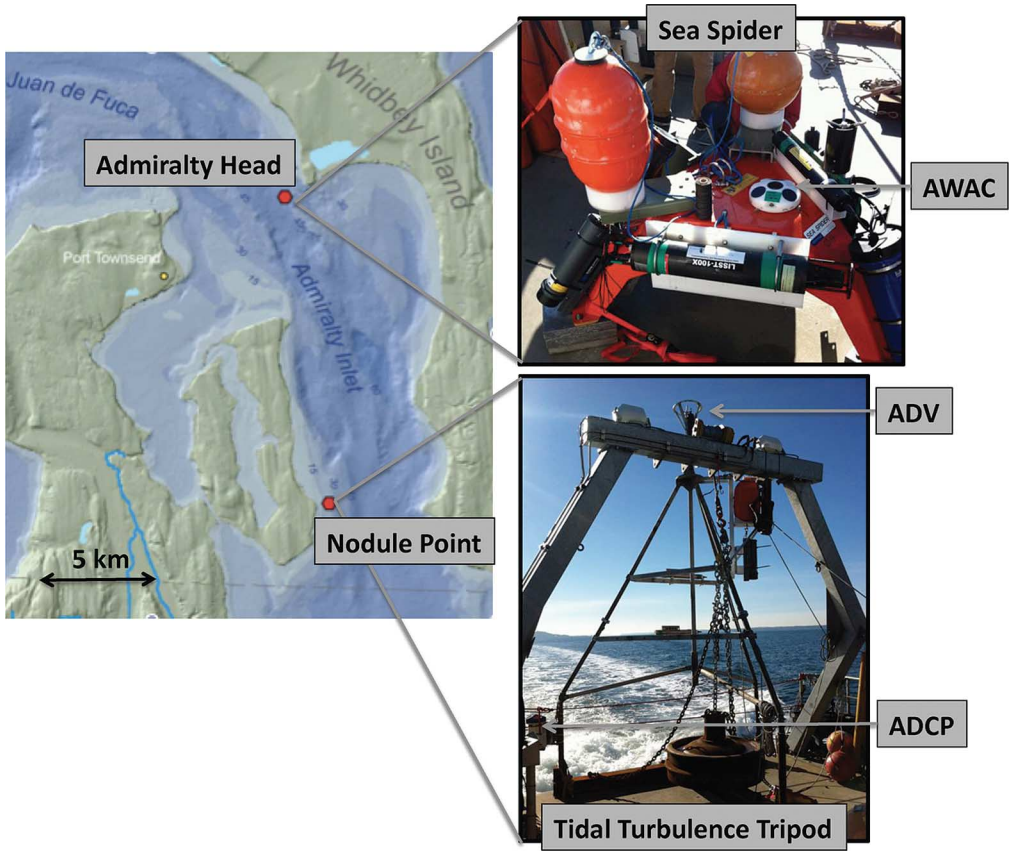

Fig. 1. Regional map, bathymetry, and locations of two tidal energy sites in Puget Sound. At Admiralty Head, a Sea Spider was deployed on the seafloor to collect AWAC data. At Nodule Point, the Tidal Turbulence Tripod was deployed on the seafloor to collect ADV and ADCP data. The Sea Spider was ballasted with 800 lb of lead (ingots), and the Tidal Turbulence Tripod was ballasted with 1800 lb of steel (railroad wheels).

the balance of tidal advection, bottom friction, and local acceleration due to the headland geometry [25], [26]. Such eddies have been shown to account for much of the form drag in a tidal channel [27], [28]. Here, these eddies are shown to dominate the turbulent inflow conditions for tidal current turbines.

III. Analysis

Data from both sites are quality controlled to remove spikes and points with low pulse correlations [29]. Data preparation is described fully in [30]. Both sites are sufficiently deep that wave orbital velocities are negligible at hub height [20], however data preparation for other sites may require isolation of wave orbital velocities using methods such as the "Z-test" [31].

The continuous time series are parsed into 5-min (300-s) windows for turbulence analysis. Five minutes was empirically determined to be the longest duration with a stable mean and variance (i.e., stationary statistics) that did not require detrending to remove the tidal signal. Longer windows can be used by removing a linear or quadratic trend, however results are sensitive to the detrending scheme and the underlying hydrodynamics may not be stationary. Windows shorter than 5 min tend to underestimate the variance because the large-scale eddies are not well captured. Data were processed using 1-, 3-, 5-, 10-, 15-, and 20-min windows before settling on the 5-min windows presented here.

For turbulence analysis, each 5-min window uses a separate principal axes decomposition to determine a mean direction $\bar{\theta}$. This is in contrast to the single principal axes decomposition used for site characterization [15], [14] and is intended to avoid contamination of the turbulence estimates by progression through the tidal ellipse. If, instead, the tidal mean direction was used, the turbulence metrics would be biased by the offset between the tidal mean and the 5-min mean. The subsequent velocity relative to this axis is analyzed for the magnitude and direction of fluctuations u' and θ', respectively.

Example time series of the hub-height speed measurements from the February deployments are shown in Fig. 2. Both the raw data horizontal u and the 5-min averages $\bar{u}$ are shown, as well as the expected Doppler noise deviation of raw data $\bar{u} \pm n$. Of course, the Doppler noise error in the 5-min averages is much less, because an ensemble of N pings, corresponding to 5 min, is used to determine $\bar{u} \pm n/\sqrt{N}$. Both sites show mixed semidiurnal tides with flows exceeding 2 m/s, as previously described by [15]. Both sites also exhibit a full range of time scales, from short turbulent fluctuations u' to the aharmonic components that disrupt the otherwise sinusoidal shape in the tidal flow $\bar{u}$.

Throughout the following analysis, horizontal speeds u are used and decomposed according to (1). Periods of "slack" flow, where $\bar{u} < 0.8$ m/s, are excluded as they are not operationally relevant for tidal turbines (i.e., below "cut-in" speed).

A. Turbulence Intensity I_u

The turbulence intensity of a flow is defined as the ratio (or percentage) of the turbulent fluctuations (typically the standard

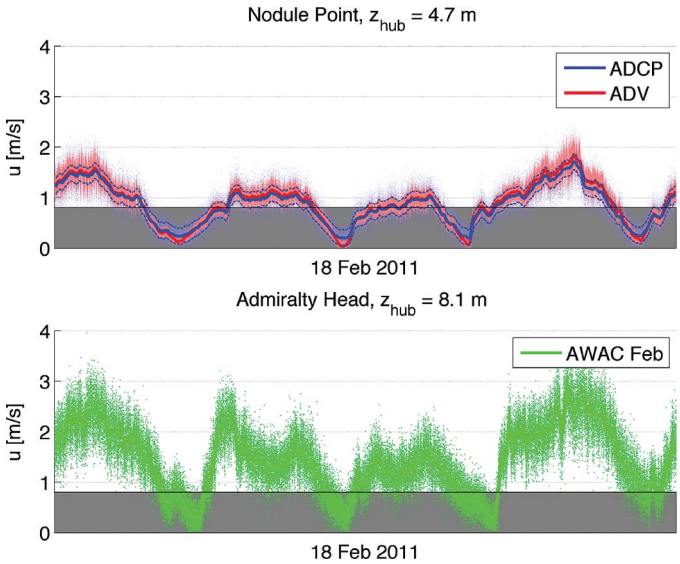

Fig. 2. Example velocity data from nominal hub heights during the February 2011 deployments at (top) Nodule Point and (bottom) Admiralty Head. Raw values are shown as points and 5-min averages are shown by the solid lines. The Doppler noise of the raw data is shown with dashed lines above and below the averages (the standard error of the averages is not shown, as it is minimal). The defined "slack" velocities are shaded in gray.

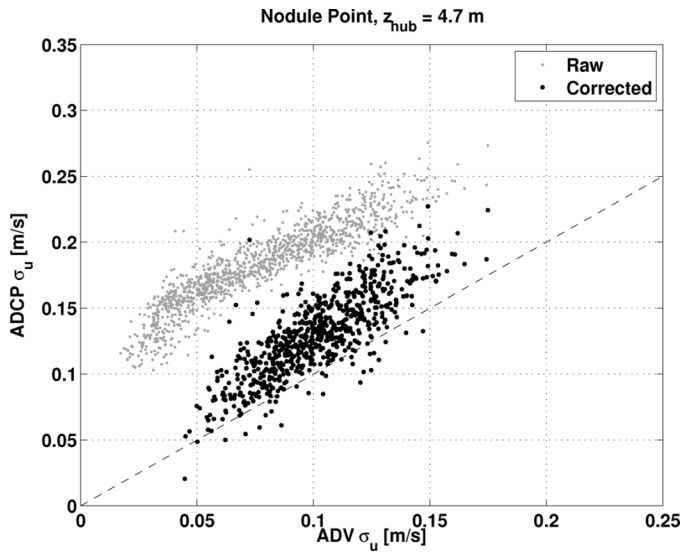

Fig. 3. Comparison of raw and corrected ADCP velocity standard deviation to ADV velocity standard deviation at the same location and height above the seabed. The dashed line indicates perfect agreement.

deviation of speed σ_u) to the mean flow. Commercial computational fluid dynamic (CFD) codes (e.g., FLUENT) and hydroelastic models used to simulate tidal turbine performance require specification of a turbulence intensity, and it is a standard metric in the wind energy industry. For acoustic Doppler measurements, a noise-corrected expression of turbulence intensity is [13]

$$I_u = \frac{\sigma_u}{\langle u \rangle} = \frac{\sqrt{\langle u'^2 \rangle - n^2}}{\bar{u}} \tag{3}$$

where the brackets indicated a time average of 5 min and $\langle u \rangle = \bar{u}$. The noise correction is valid only in the statistical sense, not as a correction to individual fluctuations. As such, it is sensitive to the number of realizations considered and Doppler noise will still result in some spreading of the corrected I_u, even in the case of a unique mean I_u [32]. This definition assumes velocity fluctuations are normally distributed; nonzero higher moments in the distribution will introduce errors.

Fig. 3 demonstrates the importance of noise correction by comparing the standard deviation of velocity $\sigma_u = \sqrt{\langle u'^2 \rangle}$ from the ADV and ADCP at Nodule Point. Before removal of Doppler noise [$\sigma_u = \sqrt{\langle u'^2 \rangle - n^2}$ as in (3)], the ADCP standard deviations are almost twice the ADV values. After correction for Doppler noise, the values are in general agreement, but notable scatter remains. This scatter suggests that the Doppler noise value n prescribed by RDI's PlanADCP™ software is an incomplete description of the measurement uncertainty. For example, Lemmin and Lhermitte [33] found that Doppler noise depends on flow speed, and Williams and Simpson [9] found RDI's PlanADCP noise values to be biased low. The incomplete removal of Doppler noise will cause resulting turbulence intensities to be biased slightly high, and thus be conservative for the purpose of tidal design specification. However, failing to account for Doppler noise at all would result in unnecessarily high factors of safety for turbine designs.

Here, we define an empirical Doppler noise as $n_e = \sqrt{\langle u'^2_{\mathrm{ADCP}} \rangle - \langle u'^2_{\mathrm{ADV}} \rangle}$, using the ADV values as ground truth. As shown in Fig. 4, the empirical values increase with flow speed, similar to the findings of [33], and are most often greater than the given PlanADCP value for speeds relevant to tidal turbines (nonslack $\bar{u} > 0.8$ m/s). The mean nonslack value is $n_e = 0.174$ m/s, compared with the PlanADCP value of $n = 0.156$ m/s. Thus, the noise-corrected turbulence intensity (3) will be biased high when using the PlanADCP value, because not all of the noise has been removed from the variance. For many deployments, it may not be practical to deploy an ADV at hub height for ground truth and then noise correction of ADCP data must rely on a prescribed value. This is the case for the Admiralty Head data set, and we use the value given by Nortek's AWAC deployment software.

Wake turbulence from the tripod is another possible source of differences between ADV and ADCP variances. While the ADV sample volume is above the tripod structure, the corresponding ADCP bin does overlap vertically with the tripod profile. Tripod wake would be preferentially biased on ebb or flood, depending on which tide had the ADCP downstream of the structure (see Fig. 1), and the data do not indicate such a bias.

Turbulence intensities are calculated for both data sets using the profile bin at hub height z_{hub}, and the resulting average I_u values are shown in Table II Mean noise-corrected turbulence intensities are around 10% for both sites and all instruments. This result is notable in similarity to many wind energy site studies. However, wind studies have shown turbulence intensities to be log-normal distributed, rather than normally distributed [1]. Thus, a better description of the mean is $\exp[\langle \ln(I_u) \rangle]$. For the distributions obtained here, the difference is negligible.

Histograms and cumulative distributions of I_u are shown in Fig. 5. Cumulative distributions for I_u without the Doppler

TABLE II
SUMMARY OF DEPLOYMENTS, AVERAGE TURBULENCE INTENSITIES, AND PEAK LENGTH SCALES

Site	Nodule Point	Nodule Point	Admiralty Head	Admiralty Head
Instrument	Nortek Vector ADV	RDI Workhorse ADCP	Nortek AWAC	Nortek AWAC
I_u [%]	8.4	11.4	11.8	9.5
I_θ [%]	4.3	7.7	6.0	5.2
L_{peak} [m]	81	72	164	152

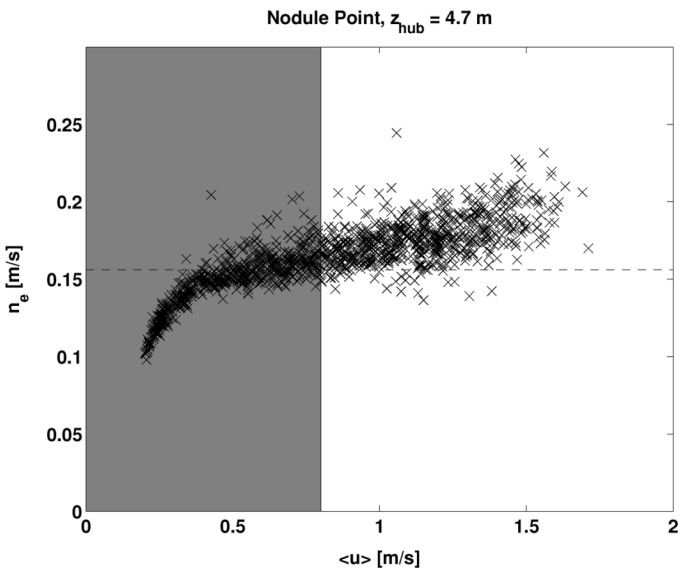

Fig. 4. Empirical Doppler noise versus mean flow speed at Nodule Point. The empirical Doppler noise is square root of the difference between the variance in the ADV velocities and the variance in the ADCP velocities from the same height above the seabed ($z_{\text{hub}} = 4.7$ m). The dashed horizontal line indicates the constant Doppler noise given by RDI's PlanADCP software, and the gray area indicates slack conditions ($\bar{u} < 0.8$ m/s).

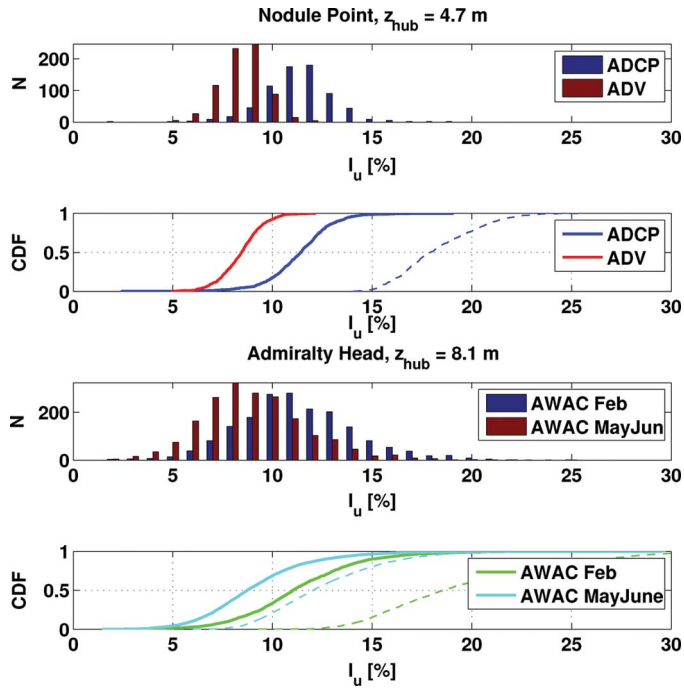

Fig. 5. Histograms (N) and cumulative distribution functions (CDFs) of turbulence intensity at Nodule Point (upper panels) and Admiralty Head (lower panels). All values are corrected for Doppler noise, except the dashed lines in the CDFs.

noise correction are also shown in Fig. 5 (and are dramatically higher). Although the noise correction in (3) improves agreement between the different measurements, there is still a bias of high I_u values from the higher noise measurements. At Nodule Point, the bias can be attributed to errors in the constant Doppler noise value $n = 0.156$ m/s from PlanADCP, as determined by comparing the cotemporal and collocated measurements (e.g., Fig. 4). At Admiralty Head, a direct comparison of independent measurements is not possible because the two data sets are of different durations and during different seasons (although both data sets span spring-neap conditions). Still, using the Doppler noise values from the Nortek AWAC software, which differed between the two deployments, gives reasonable agreement in noise-corrected turbulence intensity.

For the second deployment of the AWAC at Admiralty Head, increasing the bin size reduced the Doppler noise substantially and thus reduced the affect of noise removal. The resulting corrected turbulence intensities are slightly smaller for the second deployment, despite the reduced spatial resolution. Assuming conditions were comparable between deployments, this demonstrates both the significance of Doppler noise and the dominance of large-scale motions.

The turbulence intensities are a function of $\bar{u}$, as shown in Fig. 6, and suggest a convergence of I_u values at higher flow speeds. The turbulence intensities may be also a function of the relative position in the mixed semidiurnal tidal cycle (e.g., greater versus lesser ebb), however the data do not support a statistical distinction of turbulence intensity by the peak velocity of each cycle. At the Admiralty Head site, there is a difference in turbulence intensity by direction, with all of the larger intensities ($I_u > 25\%$) occurring on ebb. This likely is related to the nearby headland being upstream on ebb and downstream in flood [16].

B. Characteristic Fluctuation σ_c

In wind studies, the standard deviation of turbulence intensities σ_I at binned $\bar{u}$ values has been used to define a characteristic standard deviation of speed σ_c for use in turbine design, which is [1]

$$\sigma_c = (I_u + 1.29\sigma_I)\bar{u} \tag{4}$$

which is equivalent to the 90th quantile for a log-normal distribution of turbulence intensities. This is problematic for application to tidal ADCP measurements because the Doppler noise

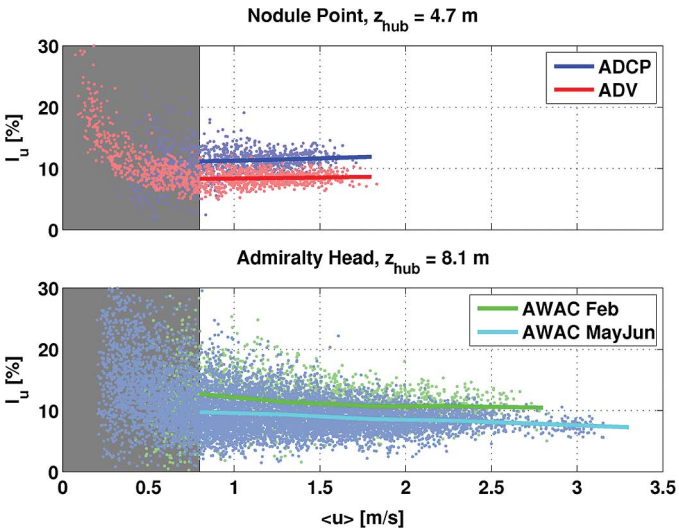

Fig. 6. Turbulence intensity versus mean speed at (top) Nodule Point and (bottom) Admiralty Head. Individual 5-min values are shown as points, and the averages at mean speed bins of 0.25 m/s are shown as solid lines. The gray area indicates slack conditions ($\bar{u} < 0.8$ m/s).

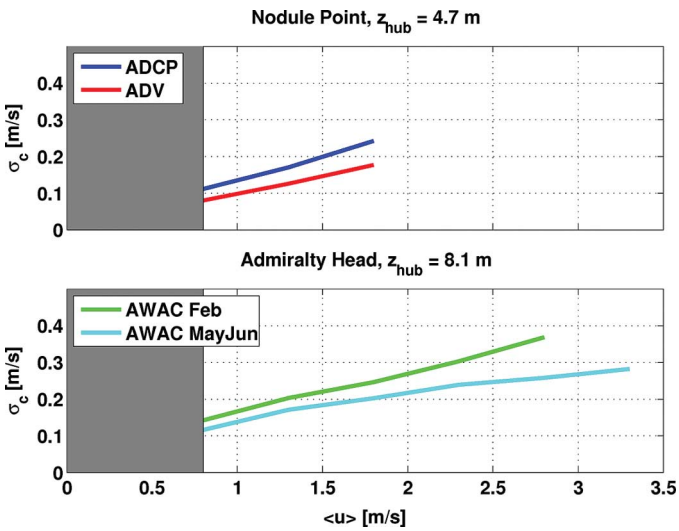

Fig. 7. Characteristic turbulent velocity fluctuation versus tidal velocity at (top) Nodule Point and (bottom) Admiralty Head. The gray area indicates slack conditions ($\bar{u} < 0.8$ m/s).

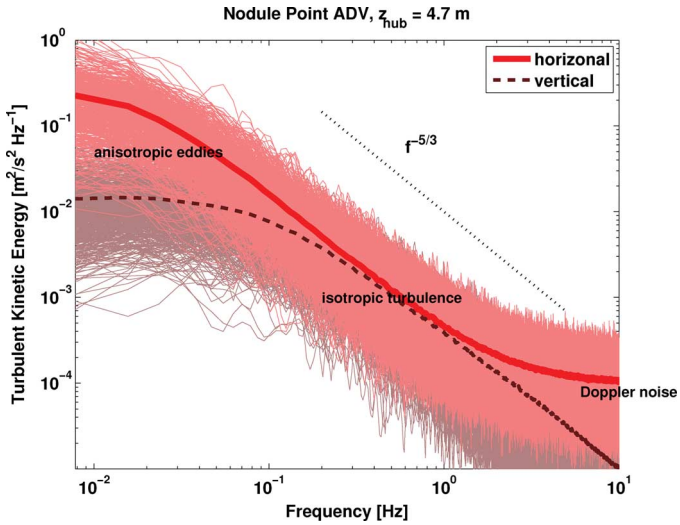

Fig. 8. Horizontal and vertical TKE versus frequency from the Nodule Point ADV. Individual spectra (5-min windows divided into four subwindows and ensemble averaged for eight degrees of freedom with frequency bandwidth $df = 0.0078$ Hz) are shown as fine lines, and the means of all spectra are shown as a thick lines. Slack periods ($\bar{u} < 0.8$ m/s) are excluded.

broadens the distribution of I_u values [32]. However, the resulting σ_c values shown in Fig. 7 are largely consistent between the ADV and the ADCP at Nodule Point and between the different AWAC deployments at Admiralty Head. In contrast to the intensities I_u, the σ_c values are not normalized and continue to increase with increasing mean speed $\bar{u}$. Further work is needed to assess the utility of the σ_c metric for tidal turbines and the appropriate model for the distribution of I_u values.

C. Time Scales: Frequency Spectra $S_{uu}(f)$

Frequency autospectra of horizontal velocities u and vertical velocities w are calculated from the ADV data at Nodule Point using four overlapping subwindows of 128 s each and shown in Fig. 8. The spectra show the TKE components as a function of frequency f, such that $\langle u'^2 \rangle = \int S_{uu}(f) df$ and $\langle w'^2 \rangle = \int S_{ww}(f) df$. (Horizontal velocity u is along the principal axis determined for each 5-min ensemble, as discussed in Section I-A.) The frequency spectra in Fig. 8 have three distinct regions: large-scale eddies at low frequencies, an isotropic eddy cascade at midfrequencies, and Doppler noise at high frequencies.

At low frequencies ($f < 0.1$ Hz), horizontal motions are far more energetic than vertical motions, consistent with large-scale anisotropic (2-D) eddies. The vertical motions likely are suppressed at these frequencies by the available water depth (see Section III-D). The low-frequency spectra are less steep than within the inertial subrange, which suggests that the large eddies may be advecting through the site without participating directly in the energy cascade (see next paragraph). Although the logarithmic axes do emphasize the low frequencies, these frequencies dominate the total TKE even when integrated over linear frequency bands. If the subwindows are extended to longer durations to observe even lower frequencies, the lowest frequencies rise toward the M4 and M6 shallow-water tidal constituents (not shown), which are known to be significant at this site [18]. Unfortunately, the low-frequency TKE, which is by far the most energetic, does not have a simple f dependence that can be exploited to derive a standard input for tidal turbines. Likely, the spectra of these large, energy-containing eddies are site-specific consequences of nearby topographic features (e.g., headlands, sills), which generate nonequilibrium upstream turbulence. Recent work suggests that general boundary layer power laws for spectra (i.e., Kaimal or Ogive curves) are commonly observed in tidal flows, however the power laws are not constrained well enough for universal application [11].

At midfrequencies ($0.2 < f < 2$ Hz), there is an inertial subrange with a classic $f^{-5/3}$ cascade [21]. As expected for isotropic (3-D) homogenous turbulence, the horizontal and vertical TKE levels are similar. This cascade transfers energy from large scales (i.e., lower frequencies) to small scales (i.e., higher frequencies), where it can be dissipated by viscosity. This cascade is used to estimate the TKE dissipation rate in Section III-F.

At high frequencies ($f > 2$ Hz), horizontal spectra become flat as a result of Doppler noise [34]. The Doppler noise is not observed for the vertical component because of the ADV beam geometry, which has a smaller projection coefficient in the coordinate transform. At slack tidal conditions ($\bar{u} < 0.8$ m/s), however, even the vertical spectra exhibit noise flattening at high frequencies (not shown). The Doppler noise can be reduced in postprocessing by assuming the noise is normally distributed and uncorrelated from the true turbulence, and then an extension of the $f^{-5/3}$ inertial subrange is observed [35]. This noise correction improves the subsequent estimation of the TKE dissipation rate (see Section III-F).

The associated ADCP and AWAC frequency spectra (not shown) have substantial Doppler noise at frequencies above 0.3 Hz, but are similar to the ADV frequency spectra at low frequencies. The large sampling volumes of the ADCP and the AWAC prohibit analysis of small scale turbulence, and thus disagreement at high frequencies is expected. In all cases, the noise level of the spectra (i.e., that flat tail at high frequencies) is consistent with a predicted $n^2/(N_{\mathrm{FFT}}df)$, which is the spectral density of the noise variance. [N_{FFT} is the number of points in the fast Fourier transform (FFP) and df is the frequency bandwidth.]

D. Length Scales: Fractional Turbulence Intensity $I_u(L)$

The frequency f spectra of horizontal TKE can be converted to horizontal length scales L using Taylor's "frozen field" assumption with an advection speed of $\bar{u}$ such that

$$L = \frac{\bar{u}}{f}. \tag{5}$$

This assumption is only valid for the frequency range of coherent motions (i.e., if the turbulence evolves faster than it is advected, the length scales will be aliased). This range could be empirically evaluated using a horizontal array of velocity measurements. However, this would be cost prohibitive for most tidal energy sites. Here, instead, we apply an *a priori* limit of horizontal length scale analysis as the distance to the shore (largest scale) and beam spread Δb of the acoustic Doppler measurement (smallest scale). The shore distances are 550 and 650 m, respectively, for Nodule Point and Admiralty Head, and the beam spreads are 2.6 and 6.8 m (see Table I). [Per (2), these beam spreads at hub height correspond to $f_s = 1.4$ Hz and $f_s = 0.5$ Hz at Nodule Point and Admiralty Head, respectively, which are within the actual $f_s = 2.0$ Hz and $f_s = 1.0$ Hz used.]

An important detail in this change of variables is the Jacobian of the transform, which gives the nonuniform length bandwidth $dL = \bar{u}f^{-2}df$, such that variance is preserved in either representation

$$\int S_{uu}(L)dL = \int S_{uu}(f)\bar{u}f^{-2}df. \tag{6}$$

The resulting spectra partition the turbulence into length scales, which can then be restricted to the scales relevant to tidal turbines.

Since the spectra S_{uu} represent the velocity variance at a particular scale, the velocity standard deviation at a particular scale is given by $\sqrt{S_{uu}}$. Thus, we can define a "fractional" turbulence intensity at each length scale as

$$i_u(L) = \frac{\sqrt{\int_{L_1}^{L_2}\left(S_{uu}(L) - \dfrac{n^2}{N_{\mathrm{FFT}}}dL\right)dL}}{\bar{u}} \tag{7}$$

where the integral over a range of lengths converts the spectral density (normalized by convention) to units of variance, and the $n^2/(N_{\mathrm{FFT}}dL)$ term corrects for the portion of Doppler noise contained in that variance (assuming uniform noise distribution, or "white" noise). Here, N_{FFT} is the number of points in the FFT, n is the Doppler noise, and a summation over all length scales regains the total turbulence intensity $I_u = \sum i_u(L)$. Thus, $i_u(L)$ is the fractional turbulent contribution at each scale of motion.

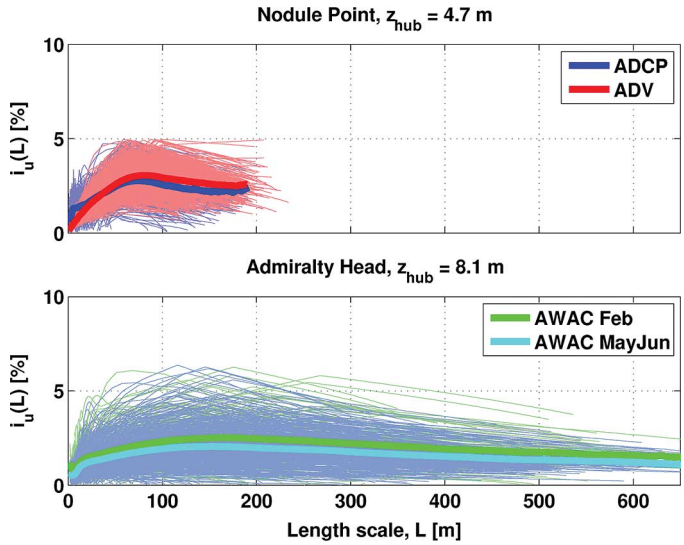

Fig. 9. Fractional turbulence intensity of horizontal motion as a function of length scale at (top) Nodule Point and (bottom) Admiralty Head. Thin lines are individual 5-min records, and thick lines are nonslack averages.

The fractional turbulence intensity from both sites and all instruments is shown in Fig. 9. As expected from the ADV frequency spectra (Fig. 8), the length dependence shows distinct regions, including a cascade of decreasing turbulence at small scales and broad region of high turbulence at large scales. The smallest scales, where Doppler noise is known to severely contaminate the observations and the sample volume is limiting, are excluded from this analysis. The dominant length scales L_{peak} for Nodule Point and Admiralty Head are approximately 75 and 150 m, respectively, and each about three times the local water depth. This is consistent with a transition from highly energetic anisotropic eddies at larger scales to an isotropic cascade at smaller scales, which are limited by either water depth or stratification. However, the peaks in $i_u(L)$ are broad and only marginally significant at the 95% confidence level, restricting any further inference on length scales dynamics.

The broad distribution of length scales is in contrast to most wind energy siting studies, which typically show a strong maxima of TKE at mesoscales and a decrease at very large scales [36]. However, the lack of a preferential turbulence scale at these sites is consistent with wind studies in areas of

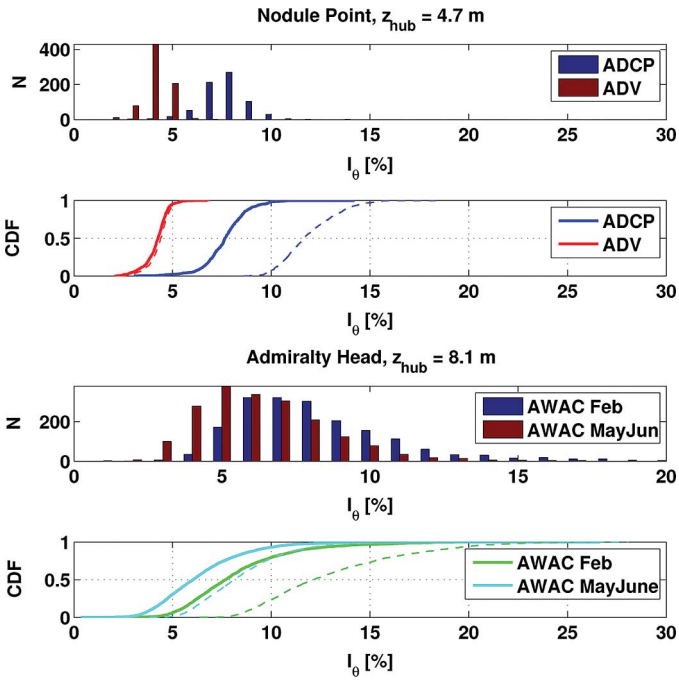

Fig. 10. Histograms (N) and CDFs of directional intensity at Nodule Point (upper panels) and Admiralty Head (lower panels). All values are corrected for Doppler noise, except the dashed lines in the CDFs.

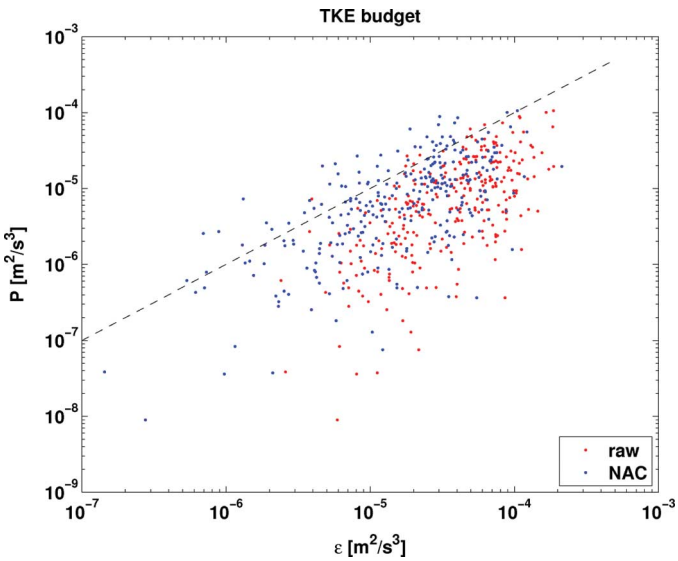

Fig. 11. Comparison of turbulent shear production rate versus dissipation rate at Nodule Point (ADV data only). The red dots are the raw spectra and the blue dots are spectra processed via noise autocorrelation.

strong topography, which are more analogous to tidal channels [40]. Here, the dominant length scales likely are related to the headland lengths and widths [25].

It is important to note the restriction of the length scale analysis to horizontal motions (Fig. 9). Determination of the horizontal velocities requires a coordinate transformation across the profiler beams, which assumes homogeneity across the beams. The beam spread at hub height Δb_{hub} is given in Table I, and may be interpreted as the minimum length scale of turbulence that is measured accurately by the profiler. Smaller scales can be resolved using the along-beam velocities, but only if those scales are isotropic and the advection by $\bar{u}$ is considered [see (5)]. For the purpose of obtaining the bulk turbulence intensities I_u, these ADCP limitations are negligible, because the larger scales set the intensity. For the purpose of examining the full turbulence spectrum, including the small scales, ADV measurements are required.

E. Directional Intensity I_θ

Fluctuations in the direction θ of tidal currents may also be important for turbine performance, and a directional turbulence intensity can be defined as

$$I_\theta = \frac{\sqrt{\langle \theta'^2 \rangle - \left(\frac{180}{\pi} \frac{n}{\bar{u}} \right)^2}}{90} \tag{8}$$

where we use the small angle approximation $\theta' \approx (180/\pi)(v'/\bar{u})$ to introduce a noise-correction term $(n/\bar{u})^2$. Raw θ' values are generally small (less than 15°), consistent with this approximation. The denominator of 90° corresponds to completely off-axis flow (i.e., perpendicular to the principal axis of the mean tidal current).

Mean directional intensity values are presented in Table II and are less than 10% for all instruments. Fig. 10 shows the histograms and cumulative distributions of the directional intensities for both sites and all instruments. Cumulative distributions for I_θ without the Doppler noise correction are also shown (and are dramatically higher). Although the noise correction improves agreement between the different measurements, there is still a trend of high I_θ values from the higher noise measurements. The trend is consistent with evaluation of an empirical Doppler noise n_e that is both higher and velocity dependent, compared with the constant value n from instrument manufacturer software.

In addition to directional fluctuations, complex rotary spectra from the ADV data can be used to examine the rotational sense of the directional variations at each frequency [37]. The rotary spectra are flat (not shown), indicating there is no dominant sense of rotation (i.e., clockwise and counterclockwise motions are equally present at all frequencies, consistent with isotropy).

F. Turbulent Kinetic Energy Budget

It is useful to examine the TKE budget to understand the dynamics of the turbulence and, eventually, improve numerical models in these regions (e.g., [38]). The full TKE budget can be written as

$$\frac{D}{Dt}(\mathrm{TKE}) + \nabla \cdot \mathcal{T} = \mathcal{P} - \epsilon \tag{9}$$

where D/Dt is the material derivative (of the mean flow), $\mathcal{T}$ is the turbulent transport, $\mathcal{P}$ is production (via shear and buoyancy), and ϵ is dissipation rate (loss to heat and sound). The production and dissipation rates are evaluated for the Nodule Point ADV data set and compared in Fig. 11. For the Admiralty Head data set, only the dissipation rate is estimated, because production estimates require either direct estimates of Reynolds stresses via ADV measurements, or inference from a four beam ADCP [7].

The dissipation rate ϵ is estimated from the ADV velocity spectra using

$$S_{ww}(f) = a\epsilon^{2/3} f^{-5/3} \left(\frac{\bar{u}}{2\pi}\right)^{2/3} \tag{10}$$

where a is a constant taken to be 0.69 for the vertical spectra. Determination of the dissipation rate is improved by removing noise from the TKE spectra using the noise autocorrelation (NAC) method [35]. The production via Reynolds stresses (from ADV data) acting on the mean shear (from ADCP data) can be estimated as

$$\mathcal{P} = -\langle u'w' \rangle \frac{d\bar{U}}{dz} \tag{11}$$

and buoyancy production is found to be negligible in this energetic, well-mixed environment. [Stratification, as measured using CTDs mounted at 1.85 and 2.55 m above the seabed, is small [<0.05 practical salinity unit (PSU) between instruments] during all nonslack conditions.] Fig. 11 shows rates of production and dissipation at Nodule Point, with scatter around a local balance (i.e., 1 : 1 line). The local balance is more prominent for dissipation rates obtained via the NAC method than for dissipation rates obtained via raw spectra [35]. For either method, there remains significant scatter around the local $\mathcal{P} - \epsilon$ balance, which suggests that transport of TKE may be important. Significant transport of TKE would be consistent with previous studies [8] and consistent with qualitative observations of eddy shedding off the nearby headland.

The dissipation rate ϵ also is estimated from the along-beam ADCP and AWAC data using the spatial structure $D(z, r)$ of the turbulence, where z is the vertical location and r is the distance between velocity fluctuations as [10]

$$D(z, r) = \langle (v'(z) - v'(z + r))^2 \rangle. \tag{12}$$

Assuming a cascade of isotropic eddies in the inertial subrange, $D(z, r)$ has the form $\mathcal{A}r^{2/3} - 2n^2$, where $\mathcal{A}$ is determined for each z and n is the Doppler noise. The dissipation rate ϵ is then calculated from [39]

$$D(z, r) = \mathcal{C}_v^2 \epsilon^{2/3} r^{2/3} \tag{13}$$

where $\mathcal{C}_v^2$ is a constant taken to be 2.1. The vertical dependence of dissipation is discussed in the following section.

G. Depth Profiles $I_u(z)$

Applying (3) at each depth bin z, a vertical dependence of turbulence intensities $I_u(z)$ is obtained and shown in Fig. 12, along with vertical profiles of the TKE dissipation rate [from (12) and (13)]. The dissipation rate is not estimated for the lowest two bins of the profile because there are not enough lag distances to evaluate (12). Both the turbulence intensities and dissipation rates decrease monotonically with elevation above the seabed, as expected for a well-developed boundary layer (i.e., "law of the wall"). At Nodule Point, where the profiles extend to the water surface, there is a reversal at the top of the profiles and an increase near the surface. This increase is expected because waves contribute additional velocity variance and wind stress forces dissipation. At Admiralty Head, where the profiles extend to less than half of the water depth (a consequence of the 1-MHz acoustic frequency of the AWAC), the turbulence intensity and dissipation trend to a constant value well above the seabed. A few profiles show a reversal, however those profiles are associated with low backscatter amplitudes (<50 counts) in the upper bins and likely are spurious. (The 1-MHz AWAC may not achieve the full 20-m range under all conditions.)

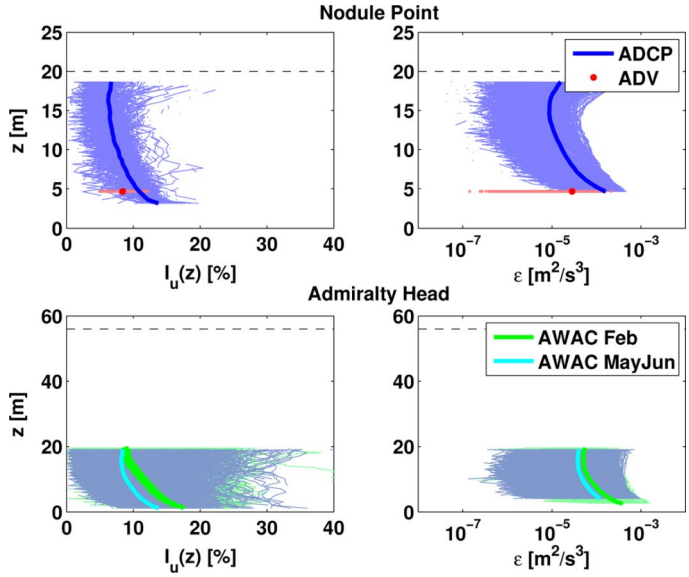

Fig. 12. Vertical profile of turbulence intensity (left panels) and dissipation rate (right panels) at Nodule Point (upper panels) and Admiralty Head (lower panels). Thin lines are individual 5-min records, thick lines are nonslack averages, and the large red dot is the ADV nonslack average. The horizontal dashed lines indicate the mean water level at the site.

An area-weighted integral of a vertical profile of turbulence intensities $I_u(z)$ can be defined as

$$\mathcal{I}_u = \frac{1}{\pi R^2} \sum \frac{I_u(z)|z - z_{\text{hub}}|(\Delta z)^2}{\sqrt{R^2 - |z - z_{\text{hub}}|^2}} \tag{14}$$

where R is the radius of a turbine. For the observations described here, there is negligible difference from the simple hub-height value.

IV. Discussion

A. Application

Accurate turbulence intensity values are important for predicting the fatigue of materials used in tidal turbines. Turbulence creates time-varying stress which will fatigue most materials more rapidly than constant stress. In the wind power industry, fatigue can be quantified using damage equivalent loads (DELs), which are evaluated for each component of a turbine and foundation [1]. The DEL is the constant load that is equivalent to the time-varying loads over a standard number of cycles (10^7 cycles at 1 Hz, for wind). A high DEL suggests a material will fail early, and thus the DEL is useful in selecting the appropriate turbine for a site. Estimation of DELs requires simulating the stress history of a material component, typically using an aeroelastic model, based on the measured turbulence intensities. For tidal turbines, the hydroelastic models necessary to simulate the stress history are still in development, and the turbulence intensity values herein can be used to initialize these models.

The distributions, or spectra, of turbulent length scales also are important to tidal turbines. From these measurements, two dynamic scales are identified: 1) large-scale eddies, which are predominantly horizontal motions at scales greater than the water depth; and 2) small-scale turbulence, which follows an isotropic cascade of decreasing energy with decreasing scale. This partitioning is approximate, because the turbulence is a continuum of motion across these scales. Still, the partitioning is useful in considering the portion of the total turbulence that may be relevant to tidal turbines. Specifically, the large scales dominate the velocity variance but may not be the critical scales for tidal turbines. More likely, tidal turbines will respond to turbulence on scales similar to the rotor diameters [O(10) m] or the blade cord lengths [O(1) m]. Band-limiting the integration of the fractional turbulence intensity (7) to the relevant length scales will provide a reduced turbulence intensity compared with the total turbulence intensity (3). This reduced turbulence will reduce the DELs, and possibly the associated costs, of turbines for a given site. More experimental and numerical work is needed to understand the structural and performance response of tidal turbines at different length scales, before this application.

Another potential application of these results is in estimation of turbine performance on short (i.e., turbulent) time scales. Given prior knowledge (from experimental or numerical studies) of turbine response as a function of frequency $R(f)$, it may be possible to predict the variation from steady power production $\bar{P} = (1/2)e\rho\bar{u^3}$ to variable power production $P(f) = R(f)(1/2)e\rho S_{uu}^{3/2}(f)$. Here, e is the turbine efficiency (which may be a function of mean speed $\bar{u}$), $S_{uu}(f)$ is the horizontal TKE, and ρ is the density of seawater. For a constant turbine response function $R(f)$, the turbine power production spectra would scale as $P(f) \approx f^{-5/2}$ over the frequency ranges of isotropic turbulence [where $S_{uu}(f) \approx f^{-5/3}$]. More likely, turbine response functions will be highly dependent on frequency, based on the geometry, mass, and generator load of a particular turbine.

B. Future Work

Major limitations in the analysis of ADCP (and AWAC) turbulence measurements are the statistical removal of Doppler noise and the restriction to length scales greater than the beam spread (or bin size, in the case of along-beam velocities). A potential future improvement to the ADCP (and AWAC) measurements would be faster sampling rates that would allow for more pings to be averaged and still obtain data at O(1) Hz. However, these faster raw sampling rates would only reduce the Doppler noise (by averaging more pings). The faster raw sampling would not allow for smaller scale analysis (because the sampling volume is still limiting).

For observations of smaller length scales or with reduced noise, ADV measurements are required. Here, ADV measurements were used to verify the successful statistical correction of Doppler noise from the ADCP measurements. A future improvement would be a hybrid instrument, using convergent beams and pulse coherence (as an ADV) on a larger scale (as an ADCP) to make precision velocity measurements at hub height from a bottom-mounted platform. This hybrid instrument would be more practical than the deployment of ADVs at turbine hub heights [O(10) m above the seabed].

Finally, future measurements also might use arrays of multiple instruments to evaluate the assumption of coherent length scales when analyzing data from a single point [i.e., (5)]. Such array measurements would further constrain the general structure of eddies at tidal energy sites. There is a clear motivation for these measurements, because coherent eddies have been shown to produce the highest stresses in wind turbines [2], [3].

V. Conclusion

This paper demonstrates the utility of ADCP (and AWAC) measurements for observing turbulence at tidal energy sites, develops a set of metrics for describing the turbulence, and presents results from two sites with pending turbine deployments. Since there have been few previous turbulence measurements at tidal energy sites, especially sites with currents above 3 m/s, the results provide some of the first realistic conditions for estimating the fatigue loads and the performance of tidal turbines.

Acknowledgment

The authors would like to thank J. Talbert and A. de Klerk for deployment (and recovery) engineering. They would also like to thank Captain A. Reay-Ellers for ship operations, and M. Taylor, A. Clifton, and several anonymous reviewers for helpful comments on the manuscript.

References

[1] S. T. Frandsen, "Turbulence and turbulence-generated structural loading in wind turbine clusters," Ph.D. dissertation, Wind Energy Dept., Tech. Univ. Denmark, Kgs. Lyngby, Denmark, 2007.

[2] N. D. Kelley and R. M. Osgood, "Using time-frequency and wavelet analysis to assess turbulence/rotor interactions," in *Proc. 19th ASME Wind Energy Symp.*, 2000.

[3] N. D. Kelley, J. Jonkman, N. Scott, J. Bialasiewicz, and L. S. Redmond, "Impact of coherent turbulence on wind turbine aeroelastic response and its simulation," Nat. Renewable Energy Lab. (NREL), Tech. Rep. CP-500-38074, 2005.

[4] H. L. Grant, R. W. Stewart, and A. Moilliet, "Turbulence spectra from a tidal channel," *J. Fluid Mech.*, vol. 12, pp. 241–268, 1961.

[5] Y. Lu and R. G. Lueck, "Using a broadband ADCP in a tidal channel. Part II: Turbulence," *J. Atmos. Ocean. Technol.*, vol. 16, pp. 1568–1579, 1999.

[6] M. T. Stacey, S. G. Monismith, and J. R. Burau, "Observations of turbulence in a partially stratified estuary," *J. Phys. Oceanogr.*, vol. 29, pp. 1950–1970, 1999.

[7] M. Stacey, "Estimation of diffusive transport of turbulent kinetic energy from acoustic Doppler current profiler data," *J. Atmos. Ocean. Technol.*, vol. 20, pp. 927–935, 2003.

[8] T. P. Rippeth, J. H. Simpson, E. Williams, and M. E. Inall, "Measurements of the rates of production and dissipation of turbulent kinetic energy in an energetic tidal flow: Red Warf Bay revisited," *J. Phys. Oceanogr.*, vol. 33, pp. 1889–1901, 2003.

[9] E. Williams and J. H. Simpson, "Uncertainties in estimates of Reynolds stress and TKE production rate using the ADCP variance method," *J. Atmos. Ocean. Technol.*, vol. 21, pp. 347–357, 2004.

[10] P. Wiles, T. P. Rippeth, J. Simpson, and P. Hendricks, "A novel technique for measuring the rate of turbulent dissipation in the marine environment," *Geophys. Res. Lett.*, vol. 33, 2006, L21608.

[11] R. K. Walter, N. J. Nidzieko, and S. G. Monismith, "Similarity scaling of turbulence spectra and cospectra in a shallow tidal flow," *J. Geophys. Res.*, vol. 116, 2011, C10019.

[12] E. Osalusi, J. Side, and R. Harris, "Structure of turbulent flow in EMEC's tidal energy test site," *Int. Commun. Heat Mass Transfer*, vol. 36, pp. 422–431, 2009.
[13] J. Thomson, B. Polagye, M. Richmond, and V. Durgesh, "Quantifying turbulence for tidal power applications," in *Proc. MTS/IEEE OCEANS Conf.*, Seattle, WA, Sep. 2010, DOI: 10.1109/OCEANS.2010.5664600.
[14] B. Polagye and J. Thomson, "Tidal energy resource characterization: Methodolgy and field study in Admiralty Inlet, Puget Sound, USA," *Proc. IMechE A, J. Power Energy*, submitted for publication.
[15] S. Gooch, J. Thomson, B. Polagye, and D. Meggitt, "Site characterization for tidal power," in *Proc. MTS/IEEE OCEANS Conf.*, Biloxi, MI, Oct. 26–29, 2009.
[16] J. Epler, B. Polagye, and J. Thomson, "Shipboard acoustic Doppler current profiler surveys to assess tidal current resources," in *Proc. MTS/IEEE OCEANS Conf.*, Seattle, WA, Sep. 2010, DOI: 10.1109/OCEANS.2010.5664387.
[17] R. Pawlowicz, R. Beardsley, and S. Lentz, "Classical tidal harmonic analysis include error estimates in MATLAB using T-TIDE," *Comput. Geosci.*, vol. 28, no. 8, pp. 929–937, 2002.
[18] B. Polagye, J. Epler, and J. Thomson, "Limits to the predictability of tidal current energy," in *Proc. MTS/IEEE OCEANS Conf.*, Seattle, WA, Sep. 2010, DOI: 10.1109/OCEANS.2010.5664588.
[19] P. MacCready and W. R. Geyer, "Advances in estuarine physics," *Annu. Rev. Mar. Sci.* vol. 2, pp. 35–38, 2010 [Online]. Available: 10.1146/annurev-marine-120308-081015
[20] C. Mei, *The Applied Dynamics of Ocean Surface Waves*, ser. Advanced Series on Ocean Engineering. Singapore: World Scientific, 1989, vol. 1, ch. 1.
[21] G. I. Taylor, "The statistical theory of isotropic turbulence," *J. Aeronaut. Sci.*, vol. 4, pp. 311–315, 1937.
[22] S. Thorpe, *An Introduction to Ocean Turbulence*. Cambridge, U.K.: Cambridge Univ. Press, 2007, ch. 1.
[23] B. H. Brumley, R. G. Cabrera, K. L. Deines, and E. A. Terray, "Performance of a broad-band acoustics Doppler current profiler," *IEEE J. Ocean. Eng.*, vol. 16, no. 4, pp. 402–407, Oct. 1991.
[24] D. Hurther and U. Lemmin, "A correction method for turbulence measurements with a 3d acoustic Doppler velocity profiler," *J. Atmos. Ocean. Technol.*, vol. 18, pp. 446–458, 2001.
[25] R. P. Signell and W. R. Geyer, "Transient eddy formation around headlands," *J. Geophys. Res.*, vol. 96, no. C2, pp. 2561–2575, 1991.
[26] W. R. Geyer and R. P. Signell, "Measurements of tidal flow around a headland with a shipboard acoustic Doppler current profiler," *J. Geophys. Res.*, vol. 95, no. C3, pp. 3189–3197, 1990.
[27] R. M. McCabe and P. MacCready, "Form drag due to flow separation at a headland," *J. Phys. Oceanogr.*, vol. 36, pp. 2136–2152, 2006.
[28] S. J. Warner and P. MacCready, "Dissecting the pressure field in tidal flow past a headland: When is form drag "real"?," *J. Phys. Oceanogr.*, vol. 39, pp. 2971–2984, 2009.
[29] S. Elgar, B. Raubenheimer, and R. T. Guza, "Quality control of acoustic Doppler velocimeter data in the surfzone," *Meas. Sci. Technol.*, vol. 16, pp. 1889–1893, 2005.
[30] M. C. Richmond, V. Durgesh, J. Thomson, and B. Polagye, "Inflow characterization for marine and hydrokinetic energy devices," Pacific Northwest Nat. Lab., Richland, WA, fy-2011: Annu. Progr. Rep., Tech. Rep. PNNL-20463, 2011.
[31] S. Elgar, B. Raubenheimer, and R. T. Guza, "Current meter performance in the surf zone," *J. Atmos. Ocean. Technol.*, vol. 18, pp. 1735–1746, 2001.
[32] B. Polagye and J. Thomson, "A leading-order noise correction for acoustic Doppler current profiler measurements at hydrokinetic energy sites," *IEEE J. Ocean. Eng.*, submitted for publication.
[33] U. Lemmin and R. Lhermitte, "Discussion of ADV measurements of turbulence: Can we improve their interpretation?," *J. Hydraulic Eng.*, vol. 125, no. 9, pp. 987–988, 1999.
[34] G. Voulgaris and J. H. Trowbridge, "Evaluation of acoustic Doppler velocimeter (ADV) for turbulence measurements," *J. Atmos. Ocean. Technol.*, vol. 15, pp. 272–289, 1997.
[35] V. Durgesh, J. Thomson, M. C. Richmond, and B. Polagye, "Noise correction of turbulent spectra obtained from acoustic Doppler velocimeters," *Flow Meas. Instrum.*, submitted for publication.
[36] E. L. Petersen, N. G. Mortensen, L. Landberg, J. Hojstrup, and H. P. Frank, "Wind power meteorology. Part 1: Climate and turbulence," *Wind Energy*, vol. 1, pp. 2–22, 1998.
[37] W. J. Emery and R. E. Thomson, *Data Analysis Methods in Physical Oceanography*. Oxford, U.K.: Pergamon, 1998, Sec. 5.6.4.1.
[38] K. Thyng, "Three-dimensional hydrodynamic modelling of inland marine waters of Washington state, United states, for tidal resource and environmental impact assessment," *IET Renew. Power Generat.*, vol. 4, no. 6, pp. 568–578, 2010.
[39] A. E. Gargett, "Velcro measurement of turbulence kinetic energy dissipation rate," *J. Atmos. Ocean. Technol.*, vol. 16, no. 12, pp. 1973–1993, 1999.
[40] A. Clifton, *Personal communication.* 2011.

Jim Thomson received the Ph.D. degree in applied ocean physics from the Massachusetts Institute of Technology/Woods Hole Oceanographic Institution joint program, Woods Hole, MA, in 2006.

Later that same year, he joined the Applied Physics Laboratory, University of Washington, Seattle. In 2009, he began a joint appointment in the Faculty of Civil & Environmental Engineering, where he teaches fluid mechanics and coastal engineering. His research program includes basic and applied ocean research, with an emphasis on field measurements of waves and currents. As a member of the Northwest National Marine Renewable Energy Center, he is applying these techniques to characterize sites for marine energy development.

Brian Polagye received the B.S.E. degree in mechanical engineering from Princeton University, Princeton, NJ, in 2000 and the Ph.D. degree in mechanical engineering from the University of Washington, Seattle, in 2009.

Since 2009, he has been a faculty member in the Department of Mechanical Engineering, University of Washington, and since 2011, the Co-Director of the Northwest National Marine Renewable Energy Center. His research interest is marine renewable energy, including resource characterization, environmental effects, and micropower for instrumentation.

Vibhav Durgesh received the B.Tech. degree in mechanical engineering from the Indian Institute of Technology (IIT), Kharagpur, India, in 1999 and the M.S. and Ph.D. degrees in mechanical engineering, with focus on experimental fluid/aerodynamics, from the University of Wyoming, Laramie, in 2004 and 2008, respectively.

Currently, he is a Research Associate at the Pacific Northwest National Laboratory, Richland, WA, with research interests in the areas of marine renewable energy and related fields.

Marshall C. Richmond received the Ph.D. degree in civil and environmental engineering from the Institute of Hydraulic Research, University of Iowa, Iowa City, in 1987.

He is a Chief Engineer in the Hydrology Group, Pacific Northwest National Laboratory (PNNL), Richland, WA. He has worked at PNNL for over 20 years. His research focuses on using computational and experimental fluid dynamics to understand the effects of hydroelectric dam operations and water quality on endangered salmon populations in the Pacific Northwest. His research projects have included: laboratory studies of the effects of fluid shear and turbulence on juvenile salmon; 3-D computational fluid dynamics (CFD) modeling of turbines, spillways, and reservoirs; water quality modeling for large river systems; and field measurements of hydrodynamic processes.